Optimizing Corn Agrivoltaic Farming through Farm-scale Experimentation and Modeling

Varsha Gupta¹, Shelby M. Gruss¹, Davide Cammarano², Sylvie M. Brouder³, Peter A. Bermel⁴, Mitchel R. Tuinstra^{3*}, Margaret W. Gitau^{1*}, Rakesh Agrawal^{5*}

¹Agricultural and Biological Engineering, Purdue University, 225 S University St., West Lafayette, 47907, Indiana, United States.

²Department of Agroecology, Aarhus University, Blichers Allé 20, Tjele, 8830, Denmark.

³Department of Agronomy, Purdue University, 915 W. State Street, West Lafayette, 47907, Indiana, United States.

⁴Birck Nanotechnology Center, Purdue University, 1205 W. State Street, West Lafayette, 47907, Indiana, United States.

^{5*}Davidson School of Chemical Engineering, Purdue University, 480 Stadium Mall Drive, West Lafayette, 47907, Indiana, United States.

*Corresponding author(s). E-mail(s): mtuinstra@purdue.edu; mgitau@purdue.edu; agrawalr@purdue.edu;

Abstract

Agrivoltaic systems, which achieve sustainable food and energy co-production (SFE) by installing photovoltaics (PVs) on farmland, offer a climate-resilient solution for meeting "full Earth" needs while adhering to land limitations. However, limited research on major row crops, such as corn ($Zea\ Mays$), constrains the widespread adoption of agrivoltaics.

To bridge this research gap, a two-step process was executed. First, extensive corn growth data was collected from neighboring regions, specifically segregating "with-PV" (shaded) and "without-PV" (unshaded) areas under real farming conditions. Using data from unshaded areas, the APSIM plant model was calibrated. Subsequently, an analytical shadow model was used to compute the spatiotemporal shadow distribution (SSD) for each row of corn between PV panels. This SSD data helped validate the APSIM model using the experimental corn yield data from shaded areas.

Next, utilizing the validated APSIM model and SSD, corn yield variations linked to PV installation geometries and tracking algorithms were simulated and examined. Power generation for each scenario was also calculated to ensure a holistic analysis. This integrated model enables the simulation of various scenarios, such as adjusting heights and other geometric characteristics of any PV installation system. For example, in our system setup, it was observed that altering the height resulted in negligible average yield variation.

In this model, for the same total radiation, it is possible to get different yield values between the plots. Therefore, correct estimation the yield requires accounting for detailed SSD. Corn yield is influenced by the spatiotemporal distribution of radiation, and consequently, SSD in addition to total radiation. This revelation highlights a potential for optimizing shadow distribution in agrivoltaic systems to simultaneously enhance crop yield and power production, potentially revolutionizing the design, management and efficiency of SFE systems.

Keywords: agriculture photovoltaic, agrivoltaic, agrophotovoltaic, PV aglectric farming, solar panels on corn belt

1 Introduction

In the face of escalating global population, economic standards, and worsening climate conditions[1], ensuring the long-term food[2, 3] and energy security[4, 5] of our planet necessitates sustainable solutions[6]. Specifically, the application of feasible sustainable energy alternatives, such as photovoltaics (PV), will likely be hampered by land availability issues[7, 8]. A potential strategy to circumvent this predicament is through the co-production of food and solar electricity on agricultural land via PV installations, known interchangeably as agrivoltaic, agrophotovoltaic, or PV aglectric (PVA) systems[8–12].

PVA farms (Fig. 1) employ PV panels whose layout and geometry, combined with the sun's position, yield a spatiotemporal shadow distribution (SSD)[8, 10, 13] that diminishes the total radiation (TR) available to plants over the growing season. The design of PV structures can also influence microclimatic conditions[14, 15]. Given that PVA farming utilizes fertile agricultural land, it is critical to mitigate any potential negative effects on food yield, necessitating an in-depth understanding of the interaction between SSD and the plants grown beneath.

Extensive research on shade-tolerant vegetables such as lettuces, cucumbers, peppers, and tomatoes has demonstrated their successful growth under PV panels[15–21]. However, a decrease in yield for potatoes, winter wheat, and some types of beans under PVA farming has been reported[22, 23]. Unfortunately, PVA studies on major row crops such as corn, soybean, and wheat under real farming conditions are almost nonexistent. According to the U.N. Food and Agriculture Organization's 2020 FAO-STAT database, these crops account for a large fraction of the farmland. For instance, in the U.S., maize and soybean are cultivated on 33 and 36 million ha, respectively, while vegetables such as lettuce only occupy 0.022 million ha. Therefore, the global-scale sustainability and implementation of PVA farming necessitate a detailed



Fig. 1 The experimental agrivoltaic farm at Purdue Agronomy Center of Research and Education (ACRE). The "with-PV" region is under the PV panels while "without-PV" regions are on far North and South sides.

analysis of solar photon sharing between PV arrays and agronomic row crops[8].

Major row crops such as corn pose challenges for PVA farming due to their incompatibility with existing PV structural layouts used for other crops. These crops are typically cultivated using tall and wide combine harvesters which are incompatible with the current short and narrow PV arrays in the existing literature [16, 18, 22, 24, 25]. Unlike non-tracking fixed PV panels, like those installed at the Fraunhofer Institute in Germany [26], east-west sun-tracking PV panels offer economic incentive for power generation and caste a dynamic shadow that shifts throughout the day. This dynamic shadow mitigates the impact of daylong shadow at a given location. The Montpellier group in France manipulated ground shadow to increase photosynthetic active radiation (PAR) on growing lettuces by anti-tracking (AT) the sun-tracking panels during morning and evening times[16]. The space between the PV rows was insufficient for the operation of a farm-scale combine harvester. To facilitate large-scale implementation of PVA farming, it is essential to generate planting data for major crops under actual farming conditions and develop validated plant and PV models. These models will elucidate the impact of PV panel design, installation, and operation on plant growth and crop yield.

Existing literature on shadow profiles and PAR intensity modeling at the plant level and their usage with crop models to predict PVA farm crop yields is limited[24, 27, 28]. Although the available models work well for PAR intensity and PV power generation, their ability to predict plant performance when combined with crop models is limited. The Montpellier group was the first to use a shadow model with a crop model for durum wheat but found contradictory results with respect to experimental observations[24]. The Fraunhofer group used idealized plant models to

understand relative plant yields for different distances between PV arrays but did not compare their calculations with experimental yields[26]. A study by Amaducci et al. simulated crop model performance for biogas maize and found that the average yield for rainfed maize in PVA farms was higher than fields without-PV[27]. However, they did not validate their model with experimental results, and our experimental findings described later contrast with theirs.

The current modeling literature lacks crop models calibrated and validated with real PVA farm data and primarily operates on coarser time scales, such as daily or seasonal. This approach fails to account for the impact of incremental dynamic shadow variation caused by tracking PV panels, observable on finer timescales like hourly variations.

This work is a comprehensive study developing PV shadow and maize models in tandem with experimental observations from a modern, mechanized corn PVA farm. The design and installation features of our east-west tracking PV panel PVA farm at Purdue University in West Lafayette, Indiana, USA (Fig. 1), extensive data collection strategies, along with critical corn yield observations are provided. A crop model, first calibrated with reference field data using full unobstructed hourly solar radiation [29], predicts the yield of the PVA farm with 2.1% accuracy. The effect of different SSDs on yield is demonstrated for a given TR, thereby emphasizing the need for light spatiotemporal distribution optimization. The impact of various PV panel heights on the SSD and the associated corn plant performance are studied through simulation. In addition, plant growth is analyzed for different tracking and anti-tracking algorithms and discuss results corresponding to various PV array densities in a PVA farm. Our study offers a systematic framework for PVA system analysis and provides some of the essential understanding needed for the optimized design, installation, and operation of PV arrays. This knowledge allows SSD manipulation during various stages of plant growth for optimal power and food production from a PVA farm, especially farms with shade-intolerant crops.

2 Purdue PVA Farm and Data Collection

The current experimental setup, as shown in (Fig. 1), at Purdue was installed in April 2019 [30]. The setup employs 4 WattSun HZLA single-axis trackers for the Sun tracking within \pm 45° east and west. The panels are oriented at -45° and 45° respectively, in reference to horizontal, beyond these bounds i.e., before the beginning and after the end of the tracking during morning and evening respectively. The dimensions of 300 W modules are 1.78m X 0.99m X 0.05m while that of 100 W modules are 0.68m X 1.01m X 0.03m. The northern half of each tracker also called contiguous panels, comprises modules placed adjacent to each other, while the southern half of each tracker row, referred to as checkerboard panels, packs modules in an alternate pattern and 0.051m away from the center. The elevation of the center of each tracker is 6.1m from the ground, and the spacing between centers of adjacent tracker rows is 9.91m. This distance is also known as the pitch. During tracking, the angle between the plane

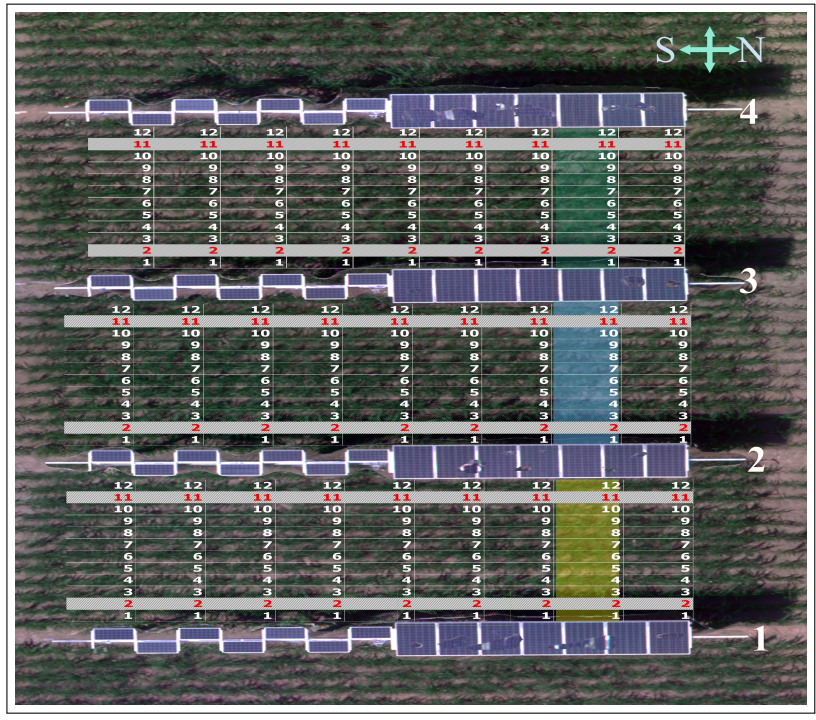


Fig. 2 The Field Layout shows 12 rows of crops between adjacent panel rows in 'with-PV' region. The panels and the rows are numbered in increasing order from east to west. Different colors represent different areas between different panel rows.

of the panel and the Direct Normal Incidence (DNI), will be referred to as offset angle. The offset angle is 90° for the experimental set-up.

For the growing season 2020, corn hybrid Pioneer 0825AM seeds were planted on 27^{th} April, and corn ears were harvested on 7^{th} October. This region where the rows of panels cast a shadow on the crops referred to as the "with-PV" region. Parallel to the "with-PV" region are running two rectangular areas on each side, i.e., North and South, where the crops receive no shadow from these PV panels. These regions collectively referred to as "without-PV" regions or the reference field as shown in Fig. 1.

Commercial PV parks generally deploy contiguous panels running parallel to each other. Therefore, this study only considers the region under contiguous panels as highlighted in (Fig. 2) in green, blue, and yellow. This area is impacted by the shadow cast due to contiguous panels only. For validation, the 12 plots highlighted in blue are considered. Corn ears of three representative plants from each of these plots were hand-collected. Overall, 570 corn plants from the "without-PV" region and 36 corn plants from the "with-PV" region respectively, were used in the analysis. The ears were cleaned, imaged, and processed using a DuPont pioneer ear photometer. The system provided approximately 40 parameters including corn yield, which is used in this study. Based on the cultivated land area and 15% moisture content, the yield obtained in

the "without-PV" region was observed to be 10,955 kg/ha while that in the "with-PV" region was 10,182 kg/ha. Please not that the yield in the "PV region" is reported based on cultivated land area only and does not include 7.7% of the uncultivated area associated with PV rows.

3 Shadow Modeling and Plant Model Validation

Solar radiation data from National Renewable Energy Laboratory (NREL) database [31] was collected for the latitude and longitude of our PV agrivoltaic farm. The hourly radiation data was used as an input to the APSIM plant model [29]. As described in Appendix A, the APSIM model was first calibrated and then validated using the "without-PV" and "with-PV" region experimental yields respectively. The calibrated APSIM model simulation result of 10,856 kg/hectare is in close agreement with the average experimental yield of 10,955 kg/hectare for the "without-PV" region. Next, as described in the supplementary information, a spatiotemporal shadow distribution model for the PV panels was developed, which is then used in conjunction with NREL radiation data to calculate hourly radiation distribution at the ground level for each plant row in the "with-PV" region throughout a day for the entire growing season. This hourly radiation data was then used as an input parameter in the calibrated APSIM model, without any further parameters adjustment within the plant model to calculate corn yield for any plant row in the PV region of interest (Fig. 2). Interestingly, the calculated average corn yield for the "with-PV" regions is 10,102 kg/hectare is in excellent agreement with the corresponding average experimental yield of 10,182 kg/hectare. This excellent agreement between the results from the crop and the SSD models and the observed experimental values gives us the confidence to explore various potential interactions between PV panels and plant performance as discussed in the next section.

4 Shadow Profile Visualization

A typical PV park consists of a large number of contiguous PV rows located equidistant from each other. Therefore, an array of twenty, unrestricted trackers- free to rotate without any bounds- loaded with contiguous PV rows (i.e. no checkerboard arrangement) with the geometric specification and field layout in our experimental setup were simulated. Here, the PV panel tracking was unrestricted i.e., it was allowed to track Sun from the Sun rise to Sun set. The resultant SSD, for a randomly selected day, July 18, 2020, between two adjacent panel rows is shown in Fig. 3. While the x-axis represents the hours of the day, the y-axis denotes plot numbers arranged in ascending order from East to West. The area between y=m and y=m+1 represents plot m+1. The plant rows are located at the East-West mid-point of the respective plot. Please note that for one-dimension in East-West direction, rows and plots can be used interchangeably. Each dark grey continuum represents the movement of the shadow due to individual PV panels, while light colors represent unshaded regions. The blue region shown in Fig. 2 simulated for these studies shall be referred to as the base case shadow profile shown in Fig. 3.

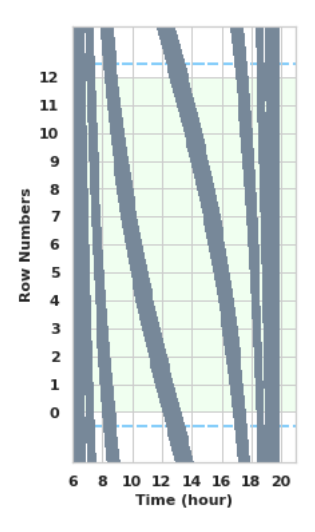


Fig. 3 Base case shadow Profile for unrestricted movement of panels. Specifications: Panel height: 6.1m, offset angle: 90° , unrestricted tracking with no AT, ground pitch: 9.91m. The blue color dashed line represents the center line of panel rows.

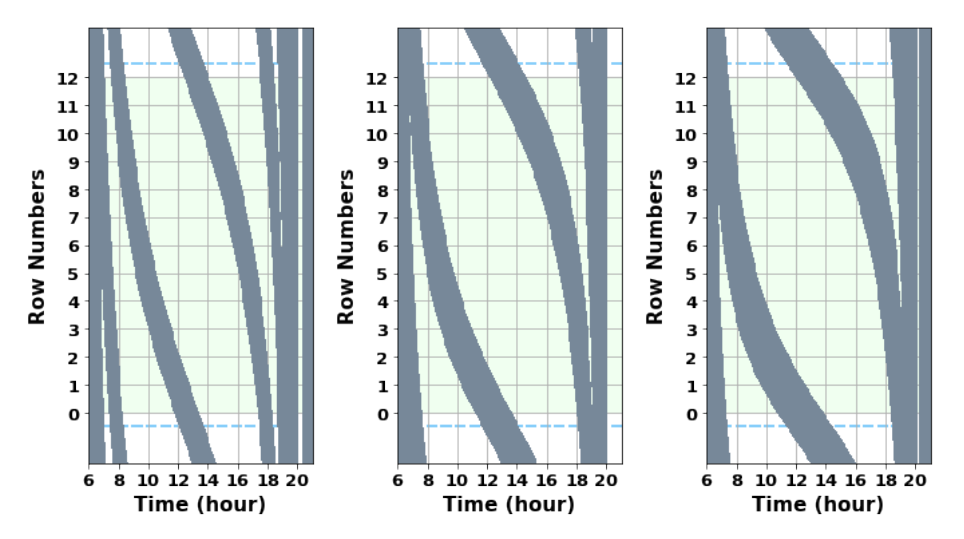
Each shadow continuum shows the SSD of the individual panels. Before solar noon, the shadows are from the panel rows that are located on the eastern side of the plot, and after the solar noon from the panel rows on the western side of the plot. While the slope of a shadow continuum indicates the speed at which the shadow moves from one location to another, the width of a shadow continuum at any point in space-time shows the residence time of the shadow at that point. At the beginning of the day, the shadow moves faster. However, as the day progresses, it slows down and stays for a longer time at any given location for a significant duration of the day before accelerating again at the end of the day.

The following set of simulations demonstrate the impact of geometrical aspects of PV panels on crop yield. The results of the simulation are applicable for the specific set of parameters mentioned for the set of simulations. Caution must be taken while extrapolating these results due to the complexity of the models involved.

5 Impact of the Height of the PV Panels

Schindel et al [22] have shown that tall PV panels contribute significantly to the cost of the PV arrays and impact the overall economics of PVA farming. Therefore, the impact of reducing PV row height on SSD was investigated. As the height of the panels decreases, the shadow tends to spread in the temporal dimension as depicted in Fig. 4. This implies that shadows stay for a longer duration at a location as the height of the panels is decreased. Three different heights i.e., 4.57m, 3.05m, and 2.44m, were simulated in addition to the base case height of 6.1m.

In this case, from the plot-wise data as shown in Fig. 5, for the same total radiation, the yield values are observed to vary between the plots. Alternately, an



 $\textbf{Fig. 4} \quad \textbf{Shadow profiles for unrestricted tracking panel height of 4.57m, 3.05m and 2.44m respectively.}$

increase in TR between the two plots does not necessarily lead to an improvement in yield. This implies that in addition to TR, one must account for the SSD to correctly estimate the yield.

Changing the height of the panels causes the shadows to rearrange in space-time dimensions such that the change in average cumulative radiation over the entire area between the adjacent PV panel rows is insignificant. The average yield of the plant rows grown under panels of different heights has no significant difference as shown in Fig. 6. Therefore, it is found that in order to reduce the fixed cost, for the specific set of heights studied here, one should consider installing panels at the shortest height possible as per the machinery and safety allowance.

6 Changing the Offset Angle

For a given set of design parameters, one can alter the operational strategy to achieve the desired trade-off between yield and solar power by adjusting the sharing of photons between the PV panels and the plants. For this set of simulations, the impact of partial tracking is studied by changing the offset angle. In this case, the shadow profiles received on the ground are compared for four different offset angles, ϕ_{tr} : 90°, 60°, 30° and 15°. For example, $\phi_{tr}=60^\circ$ means that Direct Normal Irradiance (DNI) makes an angle of 60° with the plane of the panel.

For the base case, the offset angle of 90° obstructs the maximum amount of direct light, produces maximum power, and results in minimum TR for the plants. Therefore, reducing the offset angle from 90° to 15° allows more direct light to reach the ground. Consequently, the duration of the shadow decreases gradually thereby, decreasing the thickness of the shadow in the x-direction (i.e., time) as shown in Fig. 7. This implies that at any point in time, the radiation available for biomass

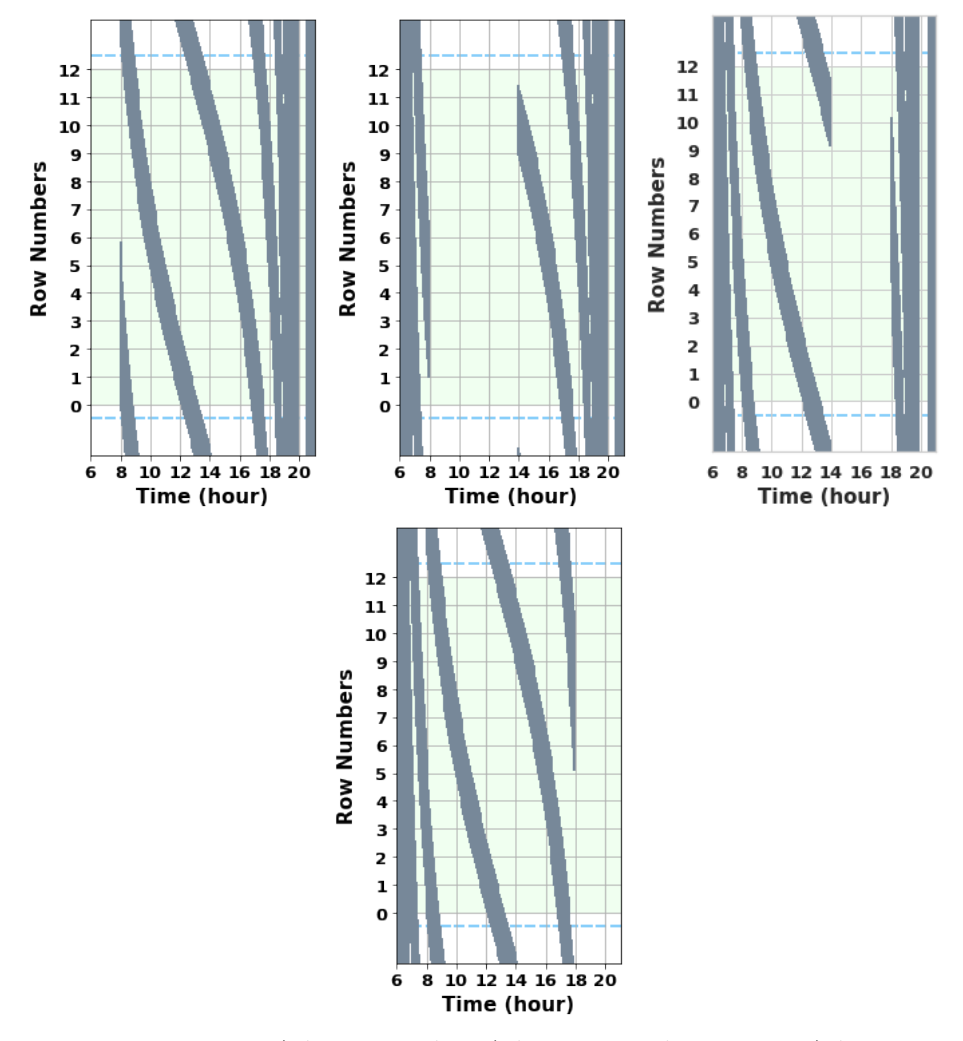


Fig. 5 Shadow profiles for a) AT before 8 AM, b) AT between 8 AM to 2 PM, c) AT 2 PM to 6 PM, and d) AT after 6 PM respectively.

fixing is more under the panels with a lower offset angle compared to that under the panels with a higher offset angle.

For different offset angles, the average yield from the validated APSIM model shows (Fig. 8) a monotonically increasing trend with respect to the total radiation for the individual rows. Moreover, since this is true for all the plots, the same is also true for average total radiation and yield values as well. It is observed that percentage change in TR exceeds the percentage change in yield, implying that gain in TR on increasing offset angle leads to higher percentage change (decrease) in power percentage than the corresponding percentage change (increase) in yield percentage.

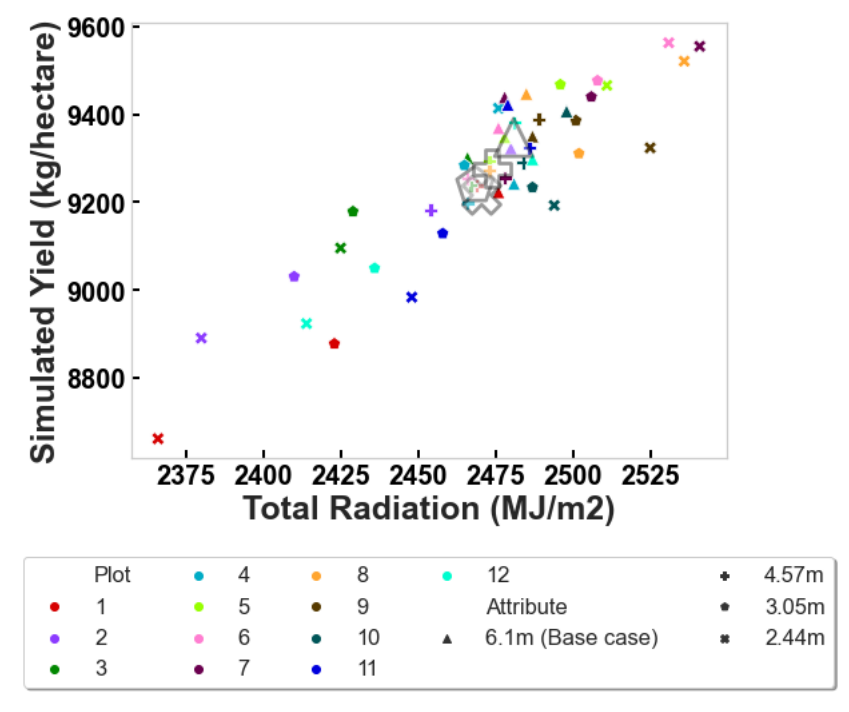


Fig. 6 Simulated yield for unrestricted tracking panels of different heights. For a given symbol, different colors represent different plots and larger gray symbols represent average yield for each set of simulated heights.

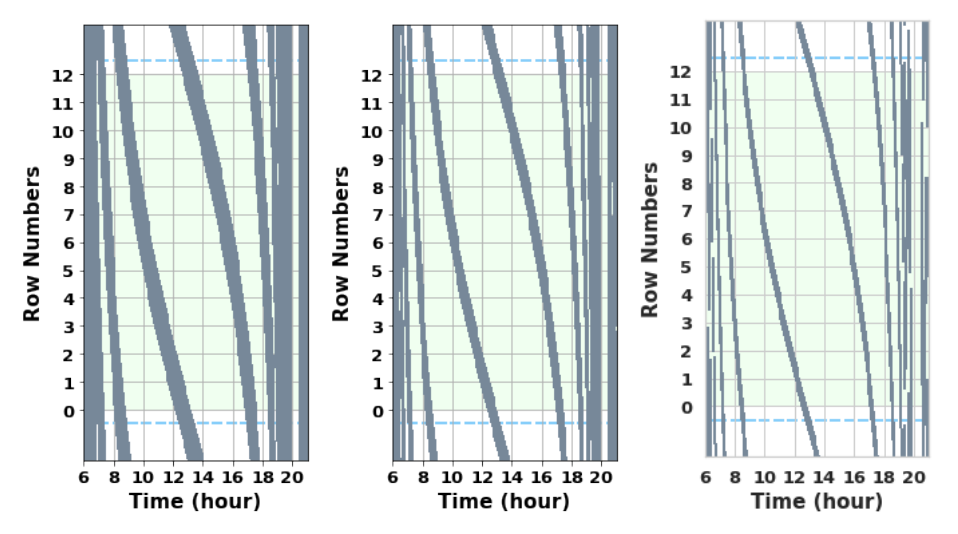


Fig. 7 Shadow profiles for unrestricted tracking at offset angles: a) 60° , b) 30° and c) 15° respectively.

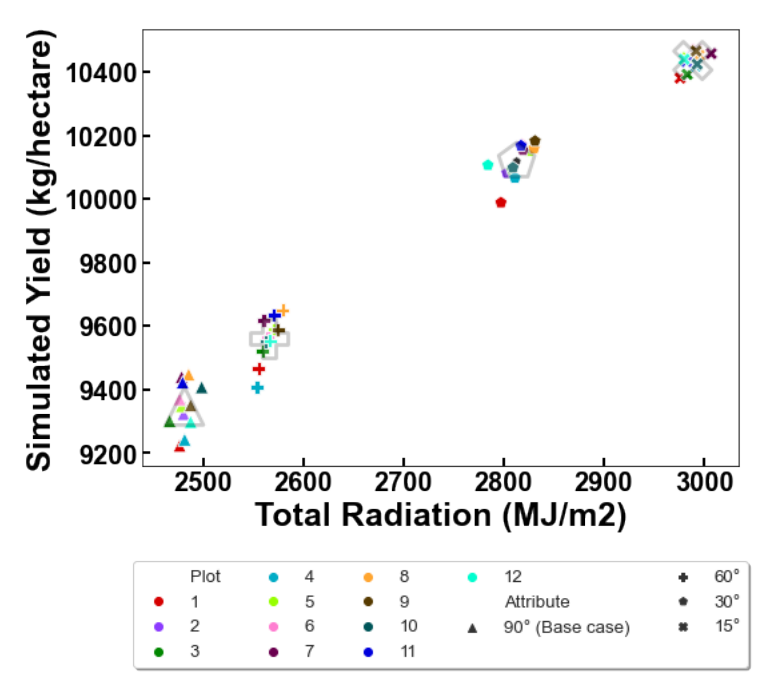
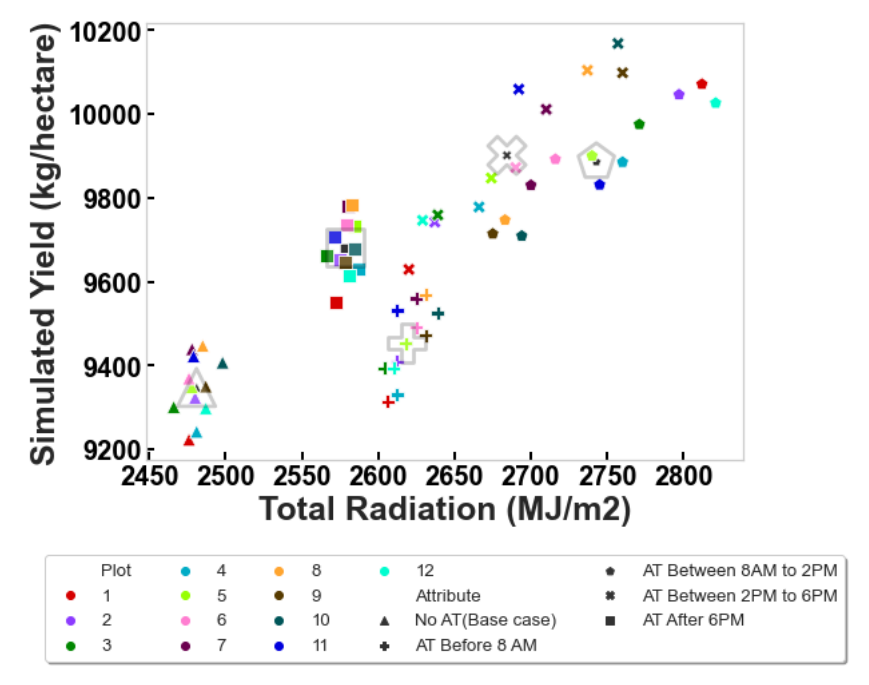


Fig. 8 Simulated yield for unrestricted tracking with offset angles of a) 90° , b) 60° , c) 30° and d) 15° .

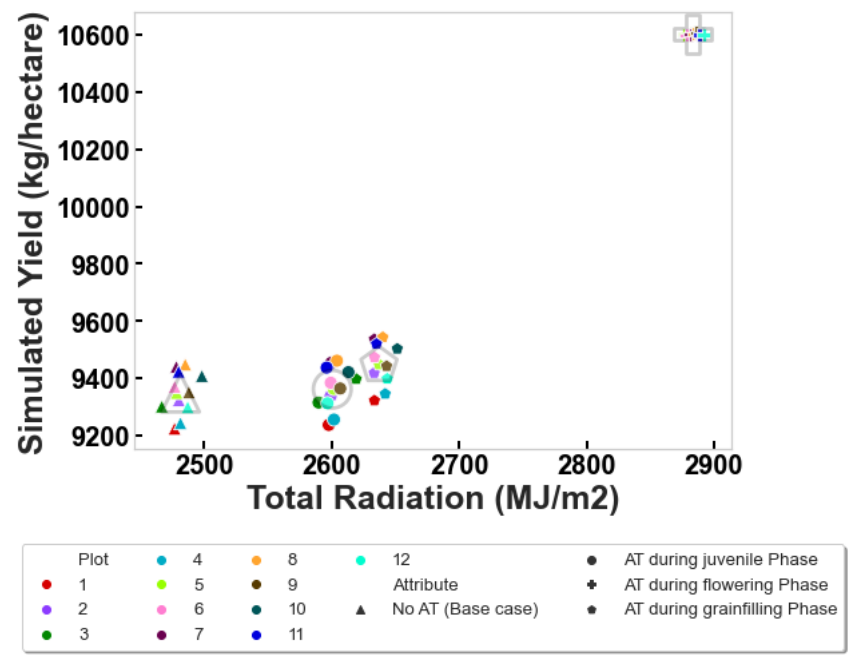
7 Impact of the Anti-tracking

For the base case, solar panels track the Sun during the entire day with an offset angle of 90°. To understand the impact of anti-tracking on crop yield, a simulation was performed with the panels anti-tracking the Sun for four different periods of time during the day: Before 8 AM, between 8 AM to 2 PM, and between 2 PM to 6 PM, and after 6 PM. This results in the corresponding shadow continuum being omitted during these parts of the day when the panels anti-track the Sun as evident from Fig. 5. For example, AT between 8 AM to 2 PM omits the shadow cast due to the east side panels and similarly, AT between 2 PM to 6 PM omits the shadow cast by the west side panel.

Introducing the shadow discontinuity by anti-tracking during different time periods of each day over the entire growing season can have an impact, albeit modest, on the plant yield as shown in Fig. 9. AT during early morning and late evening cause the cumulative radiation for the plants to increase by approximately 5.2% and 3.8% respectively. This causes the growing season power production to reduce by 7% and 4.9% respectively. However, the corresponding change in average yield for both cases is 1.1% and 3.4%. AT 6 hours before the solar noon and 4 hours after the solar noon lead to an increase in cumulative radiation by 9.5% and 7.6% respectively. While the respective growing season power production goes down by 41.1% and 24.5%. The



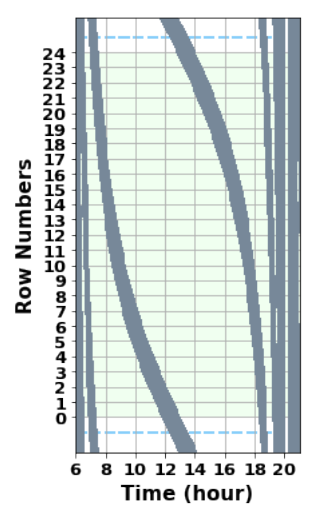
 $\textbf{Fig. 9} \ \ \text{Simulated Yield for unrestricted tracking panels with anti-tracking (AT) during different parts of the day. } \\$



 ${f Fig.~10}$ Simulated yield for restricted tracking panels with anti-tracking (AT) during different parts of the growing season.

resultant improvement in average yield is by only 5.4% and 5.6% respectively.

Instead of anti-tracking during the entire growing season, anti-tracking was explored over the entire day during juvenile, flowering or grain-filling seasons. Anti-tracking during juvenile, flowering and grain-filling seasons have different effects on yield. While anti-tracking during the juvenile phase does not have pronounced effects on both radiation and yield as shown in Fig. 10. Anti-tracking during flowering and grain-filling causes an increased TR by 13.9% and 5.9% respectively. The growing season power generation decreases by 45.6% and 16.8% respectively. The improvement in yield value obtained on anti-tracking during flowering and grain filling stages are 11.8% and 1% respectively. This implies that AT during flowering may lead to significant improvement in yield and provides an average corn yield that is similar to the one from the "without-PV" farming region.



 ${\bf Fig.~11~~Shadow~Profile~for~unrestricted~tracking~for~double~pitch}$

8 Impact of Doubling the Distance between the PV Arrays

The inclusion of a double pitch between two adjacent PV rows, compared to the base case, allows for the spread of shadow spatially. As shown in Fig. 11, the shadow profile for each pitch remains continuous.

Introducing more area between adjacent PV rows causes the rows to separate in terms of total radiation received on the ground. On doubling the distance between the adjacent PV rows, the cumulative radiation on the area between the two adjacent PV rows increases by 11%. This causes an increase in yield by 7% as shown in Fig. 12.

However, it is interesting to compare this case with a second case where half the land is populated with-PV panels at a distance of the base case pitch, and the remaining half is used for regular agricultural farming. Simulating these two scenarios reveal similar corn yield. Since both cases use the same amount of total land and produce the same power from the cost perspective, the second case is likely preferable and shows increasing pitch between adjacent PV rows beyond that for the base case is likely to be not advantageous. Increasing the distance between the adjacent PV rows will likely use more copper wires that will need to be run over larger distances contributing to an increase in cost.

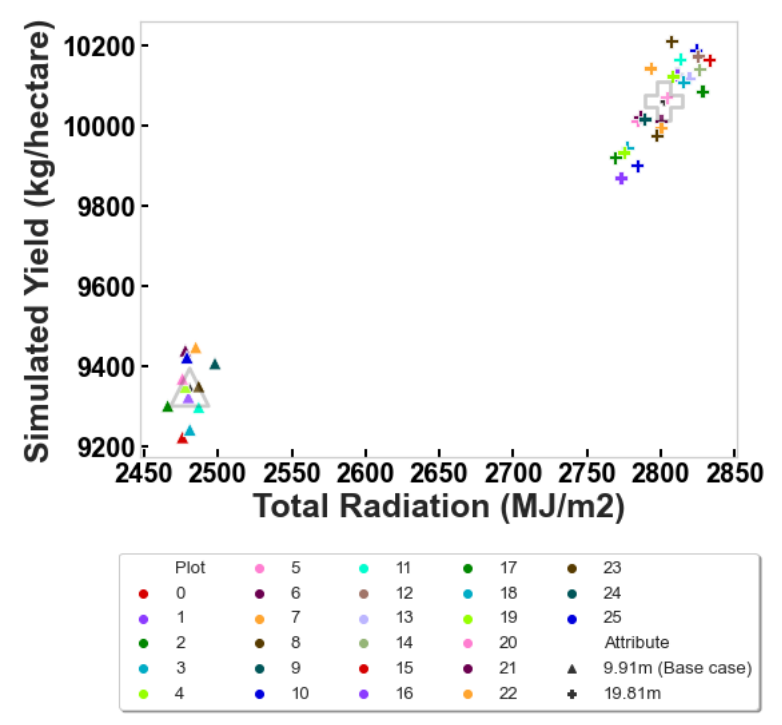


Fig. 12 Yield for unrestricted tracking for base case pitch $(9.91 \mathrm{m})$ and double pitch $(19.81 \mathrm{m})$ respectively.

9 Conclusion

Extensive corn yield data under dynamic shadows from east-west Sun tracking PV panels has been collected herein. The installation of PV panels and crop growth is done at a scale to replicate actual farming practices for corn. The corn yield from the adjoining farming area without-PV was measured to be 10,955 kg/hectare, compared to the yield of 10,182 kg/hectare of the planted area between the PV panels.

APSIM, a crop model, was calibrated using corn yield data for the adjoining area farming without any PV installation. For this purpose, hourly solar irradiation for each day during the entire growing season was an input parameter. The corn yield of 10,856 kg/hectare of the cultivated area from the calibrated APSIM model was in good agreement with the experimental value of 10,955 kg/hectare. A shadow model was used in conjunction with the available hourly radiation data to calculate the calculate hourly radiation available for each corn row growing underneath the tracking solar panels. The spatiotemporal radiation distribution was then used as an input parameter to the calibrated APSIM model and the calculated 10,102 kg/hectare corn yield was found to be in remarkable agreement with the experimental yield for the "with-PV" region of 10,182 kg/hectare.

With the remarkable agreement between the experimental crop yield from the PVA farm and our simulation models, a number of interesting questions associated with the design, installation, and operation of the solar panels could be explored. First, it is found that designs that lower the PV panel height without impeding the movement of plant machinery should be envisioned as the overall average corn yield is a weak function of the PV panel height up to 2.44m. However, the variability from one corn row to other increases as the PV panel height is reduced. Anti-tracking during certain periods of the day for the entire growing season was considered as a means to increase the radiation available to the plants. It was found that anti-tracking around solar noon, i.e., from 2 PM to 6 PM provided the greatest increase in the corn yield, however, this increase in corn yield of 5.6% is quite modest and should be weighed against a substantial decline in solar power. All-day anti-tracking during different stages of plant growth was also explored. Among the three stages considered, juvenile flowering and grain-filling, it is found that anti-tracking is most effective during the flowering period and provides an average corn yield that is similar to the one from the "without-PV" farming region. This corn yield advantage needs to be considered in the context of minimal power from PV panels during the flowering stage of plant growth. Another interesting finding is that for our PV module sizes, increasing the distance between the adjacent PV rows beyond the 9.1m, while keeping the total power over the entire land constant, does not lead to an increase in corn yield based on the total land area. In conclusion, the total radiation received by plants during the growing season does not always exhibit a direct relationship with yield. Instead, in addition to TR, accounting for SSD is critical to discern the exact variation in crop growth dynamics.

Acknowledgments

The authors would like to thank all National Science Foundation (NSF) Research Trainee Program (NRT) cohort Elizabeth K. Grubbs, Daniel Hayes, Anna Murray, Apurva Pradhan, David Rokke, Val Z. Schull, Jonathan Turnley, and Kyle Weideman for their valuable assistance with plot layout, field data collection, and hand

harvesting, and financial support from NSF grants 1735282 and 1855882 is gratefully acknowledged.

References

- [1] Hanse, J.E., Sato, M.: Trends of measured climate forcing agents. Proceedings of the National Academy of Sciences 98, 14778–14783 (2001)
- [2] Tilman, D.: Food and health of a full earth. Daedalus 144, 5–7 (2015)
- [3] Wheeler, T., Braun, j.V.: Climate change impacts on global food security. Science **341**(6145), 508–513 (2013). https://doi.org/10.1126/science.1239402
- [4] Van Ruijven, B.J., De Cian, E., Sue Wing, I.: Amplification of future energy demand growth due to climate change. Nature communications **10**(1), 1–12 (2019)
- [5] Caldeira, K., Jain, A.K., Hoffert, M.I.: Climate sensitivity uncertainty and the need for energy without co2 emission. Science 299(5615), 2052–2054 (2003) https://www.science.org/doi/pdf/10.1126/science.1078938. https://doi. org/10.1126/science.1078938
- [6] Dincer, C. I.and Acar: A review on clean energy solutions for better sustainability.
 International Journal of Energy Research 39, 585–606 (2015). https://doi.org/10.1002/er.3329
- [7] Capellán-Pérez, I., De Castro, C., Arto, I.: Assessing vulnerabilities and limits in the transition to renewable energies: Land requirements under 100% solar energy scenarios. Renewable and Sustainable Energy Reviews 77, 760–782 (2017)
- [8] Miskin, C.K., Li, Y., Perna, A., Ellis, R.G., Grubbs, E.K., Bermel, P., Agrawal, R.: Sustainable co-production of food and solar power to relax land-use constraints. Nature Sustainability 2, 972–980 (2019). https://doi.org/10.1038/s41893-019-0388-x
- [9] Dupraz, C., Marrou, H., Talbot, G., Dufour, L., Nogier, A., Ferard, Y.: Combining solar photovoltaic panels and food crops for optimising land use: Towards new agrivoltaic schemes. Renewable energy 36(10), 2725–2732 (2011)
- [10] Amaducci, S., Yin, X., Colauzzi, M.: Agrivoltaic systems to optimise land use for electric energy production. Applied energy 220, 545–561 (2018)
- [11] Gençer, E., Miskin, C., Sun, X., Khan, M.R., Bermel, P., Alam, M.A., Agrawal, R.: Directing solar photons to sustainably meet food, energy, and water needs. Scientific reports **7**(1), 3133 (2017)
- [12] Weselek, A., Ehmann, A., Zikeli, S., Lewandowski, I., Schindele, S., Högy, P.: Agrophotovoltaic systems: applications, challenges, and opportunities. a review. Agronomy for Sustainable Development **39**, 1–20 (2019)
- [13] Riaz, M.H., Imran, H., Younas, R., Butt, N.Z.: The optimization of vertical

- bifacial photovoltaic farms for efficient agrivoltaic systems. Solar Energy 230, 1004–1012 (2021)
- [14] Marrou, H., Guilioni, L., Dufour, L., Dupraz, C., Wery, J.: Microclimate under agrivoltaic systems: Is crop growth rate affected in the partial shade of solar panels? Agricultural and Forest Meteorology 177, 117–132 (2013)
- [15] Barron-Gafford, G.A., Pavao-Zuckerman, M.A., Minor, R.L., Sutter, L.F., Barnett-Moreno, I., Blackett, D.T., Thompson, M., Dimond, K., Gerlak, A.K., Nabhan, G.P., et al.: Agrivoltaics provide mutual benefits across the food—energy—water nexus in drylands. Nature Sustainability 2(9), 848–855 (2019)
- [16] Valle, B., Simonneau, T., Sourd, F., Pechier, P., Hamard, P., Frisson, T., Ryckewaert, M., Christophe, A.: Increasing the total productivity of a land by combining mobile photovoltaic panels and food crops. Applied energy 206, 1495–1507 (2017)
- [17] Marrou, H., Wéry, J., Dufour, L., Dupraz, C.: Productivity and radiation use efficiency of lettuces grown in the partial shade of photovoltaic panels. European Journal of Agronomy 44, 54–66 (2013)
- [18] Weselek, A., Bauerle, A., Hartung, J., Zikeli, S., Lewandowski, I., Högy, P.: Agrivoltaic system impacts on microclimate and yield of different crops within an organic crop rotation in a temperate climate. Agronomy for Sustainable Development 41(5), 59 (2021)
- [19] Marrou, H., Dufour, L., Guilioni, L., Salles, J.-M., Loisel, P., Nogier, A., Wéry, J.: Designing farming systems combining food and electricity production. Gansu Science and Technology Press (2013)
- [20] Dinesh, H., Pearce, J.M.: The potential of agrivoltaic systems. Renewable and Sustainable Energy Reviews **54**, 299–308 (2016)
- [21] Al Mamun, M.A., Dargusch, P., Wadley, D., Zulkarnain, N.A., Aziz, A.A.: A review of research on agrivoltaic systems. Renewable and Sustainable Energy Reviews 161, 112351 (2022)
- [22] Schindele, S., Trommsdorff, M., Schlaak, A., Obergfell, T., Bopp, G., Reise, C., Braun, C., Weselek, A., Bauerle, A., Högy, P., et al.: Implementation of agrophotovoltaics: Techno-economic analysis of the price-performance ratio and its policy implications. Applied Energy 265, 114737 (2020)
- [23] Santra, P., Meena, H.M., Yadav, O.: Spatial and temporal variation of photosynthetic photon flux density within agrivoltaic system in hot arid region of india. Biosystems Engineering **209**, 74–93 (2021)
- [24] Dupraz, C., Talbot, G., Marrou, H., Wery, J., Roux, S., Liagre, F., Ferard, Y.,

- Nogier, A.: To mix or not to mix: evidences for the unexpected high productivity of new complex agrivoltaic and agroforestry systems. In: Proceedings of the 5th World Congress of Conservation Agriculture: Resilient Food Systems for a Changing World (2011)
- [25] Gonocruz, R.A., Nakamura, R., Yoshino, K., Homma, M., Doi, T., Yoshida, Y., Tani, A.: Analysis of the rice yield under an agrivoltaic system: A case study in japan. Environments 8(7), 65 (2021)
- [26] Fraunhofer, I.: Harvesting the sun for power and produce—agrophotovoltaics increases the land use efficiency by over 60 percent. Fraunhofer ISE: Freiburg, Germany (2017)
- [27] Amaducci, S., Yin, X., Colauzzi, M.: Agrivoltaic systems to optimise land use for electric energy production. Applied energy **220**, 545–561 (2018)
- [28] Trommsdorff, M., Kang, J., Reise, C., Schindele, S., Bopp, G., Ehmann, A., Weselek, A., Högy, P., Obergfell, T.: Combining food and energy production: Design of an agrivoltaic system applied in arable and vegetable farming in germany. Renewable and Sustainable Energy Reviews 140, 110694 (2021)
- [29] Holzworth, D.P., Huth, N.I., deVoil, P.G., Zurcher, E.J., Herrmann, N.I., McLean, G., Chenu, K., van Oosterom, E.J., Snow, V., Murphy, C., et al.: Apsim-evolution towards a new generation of agricultural systems simulation. Environmental Modelling & Software 62, 327–350 (2014)
- [30] Perna, A., Grubbs, E.K., Agrawal, R., Bermel, P.: Design considerations for agrophotovoltaic systems: maintaining pv area with increased crop yield. In: 2019 IEEE 46th Photovoltaic Specialists Conference (PVSC), pp. 0668–0672 (2019). IEEE
- [31] NSRDB: National Solar Radiation Database. https://maps.nrel.gov/nsrdb-viewer. Accessed: 2021-12-09